Genome-Wide Analysis of the *Fusarium oxysporum mimp* Family of MITEs and Mobilization of Both Native and De Novo Created *mimps*

Mara Bergemann · Olivier Lespinet ·
Sarrah Ben M'Barek · Marie-Josée Daboussi ·
Marie Dufresne

Abstract   We have performed a genome-wide analysis of the *mimp* family of miniature inverted-repeat transposable elements, taking advantage of the recent release of the *F. oxysporum* genome sequence. Using different approaches, we detected 103 *mimp* elements, corresponding to 75 nonredundant copies, half of which are located on a single small chromosome. Phylogenetic analysis identified at least six subfamilies, all remarkably homogeneous in size and sequence. Based on high sequence identity in the terminal inverted repeats (TIRs), *mimp* elements were connected to different *impala* members. To gain insights into the mechanisms at the origin and amplification of *mimps*, we studied the potential of *impala* to cross-mobilize different *mimps*, native but also created de novo by inserting a short DNA segment between two TIRs. Our results show that TIR sequences are the main requirement for mobilization but that additional parameters in the internal region are likely to influence transposition efficiency. Finally, we show that integration site preference of native versus newly transposed *mimps* greatly varies in the host genomes used in this study.

M. Bergemann · O. Lespinet · S. B. M'Barek · M.-J. Daboussi ·
M. Dufresne (✉)
Institut de Génétique et Microbiologie, Université Paris-Sud 11,
CNRS, UMR8621, 91405 Orsay, France
e-mail: marie.dufresne@igmors.u-psud.fr

S. B. M'Barek
Plant Research International B.V., P.O. Box 16,
6500 AA Wageningen, The Netherlands

transposed *mimps* greatly varies in the host genomes used in this study.

Introduction

Class II transposable elements (TEs), also called DNA transposons, have terminal inverted repeats (TIRs) at both ends and transpose using a "cut-and-paste" mechanism. This process involves cleavage at the ends of the transposon and strand transfer that allows excision of the element prior to its reinsertion at another locus in the genome. This mechanism is performed by a transposase encoded by autonomous elements which, after specific binding of the enzyme at the ends of the element, catalyzes the steps mentioned above. Class II TEs are either autonomous transposons encoding their own transposase or nonautonomous elements corresponding to mutation (mostly deletion) derivatives of the previous ones. Although not encoding for a functional transposase, most nonautonomous elements can still be mobilized by a transposase provided *in trans*, because of strong sequence similarity, in particular, in the TIRs region.

Miniature inverted-repeat transposable elements (MITEs) are short (<500-bp) elements, structurally similar to defective class II elements. In particular, they are characterized by the presence of TIRs. They also share other features that distinguish them from other nonautonomous DNA transposons such as a high copy number and size homogeneity (Feschotte et al. 2002). With the progress of large-scale sequencing, it has become apparent that

MITEs are important components of eukaryotic genomes. First identified in plants (Wessler et al. 1995), they have been subsequently found, generally in large copy numbers, in a wide range of animal and fungal genomes (for a review, see Feschotte et al. 2002). Similarity searches based on TIR sequences have allowed the identification of autonomous class II elements, potentially responsible for the mobilization of MITEs (Feschotte and Mouches 2000; Feschotte et al. 2003; Jiang et al. 2003; Kikuchi et al. 2003; Macas et al. 2005; Saito et al. 2005; Quesneville et al. 2006). However, only a few recent studies have demonstrated, either by in vitro biochemical approaches (Loot et al. 2006; Feschotte et al. 2005) or in vivo (Yang et al. 2007; Dufresne et al. 2007), that class II transposases do have the potential to mobilize MITEs.

Recent genome-wide analyses have greatly improved our knowledge on MITE families, however, many questions remain about their origin and amplification. Some MITEs may have originated by deletion of autonomous class II elements (Feschotte and Mouches 2000; Jiang et al. 2003; Ramussen et al. 2004), as shown by extended regions of similarity to coexisting TEs. Other MITE families may rather originate de novo by fortuitous juxtaposition of sequences resembling the TIRs of autonomous elements (Feschotte et al. 2002; Quesneville et al. 2006).

In *Fusarium oxysporum,* numerous TEs belonging to all structural classes have been identified (Daboussi and Capy 2003). The *impala* family of DNA transposons belonging to the *Tc1/mariner* superfamily has been extensively studied in our laboratory (Hua-Van et al. 1998, 2001a, b). This family occurs at a low copy number in *F. oxysporum* and comprises at least five different subfamilies, which differ by a high level of nucleotide diversity (Hua-Van et al. 1998, 2001a). Inactive elements, representing the majority of *impala* copies, were identified in all subfamilies, in contrast with autonomous elements, encountered only in subfamilies *E* and *D* (Hua-Van et al. 1998, 2001a, b). Two short elements (∼200 bp) displaying TIRs very similar to those of *impalaE* have been recognized in the genome of *F. oxysporum* (Hua-Van et al. 2000). These elements, called *mimp1* and *mimp2*, exhibit features of MITEs. Recently, we demonstrated that *mimp1* is mobilized through the action of the *impalaE* transposase (Dufresne et al. 2007).

In this paper, we extract *mimp*-like elements from the recently available genome sequence of *F. oxysporum* and classify them into different subfamilies. We analyze their chromosomal distribution and insertion sites relative to predicted genes. We also demonstrate the mobilization of a native *mimp* element belonging to another subfamily than *mimp1*. More interestingly, we show that a *mimp* element created in vitro can also be mobilized by the *impalaE* transposase.

Materials and Methods

Fungal Strains

The *Fusarium oxysporum* strains FOM24 (*F. oxysporum* f.sp. *melonis*) and FOL15 (*F. oxysporum* f.sp. *lycopersici*) were used in polymerase chain reaction (PCR) experiments either to identify novel *mimp* elements (both strains) or to generate the internal sequence of the de novo created *mimp*Nia element (FOM24 strain). The *F. graminearum* nitrate reductase-deficient mutant Fg820*nia5* was used as a recipient strain in all transformation experiments. Fg820*nia5* and derivatives were grown on PDA plates. To obtain spores, flasks or 2-ml Eppendorf tubes containing 20 ml or 1 ml of liquid mung bean medium (Bai and Shaner 1996), respectively, were inoculated with a plug from an 8-day-old PDA plate and incubated with moderate shaking at 26°C for 2–5 days. For long-term storage, a plug of the culture was put on 500 µl PDA poured in a 2-ml Eppendorf tube and, after growth for 2–3 days at 26°C, was stored at 4°C.

Plasmids and Constructs

pHEO62 contains the open reading frame (ORF) encoding the *impalaE* transposase (Hua-Van et al. 1998), cloned between the *gpdA* promoter and the *trpC* terminator of *Aspergillus nidulans.* It also carries a cassette conferring hygromycin resistance from the pBC1004 plasmid (Carroll et al. 1994), which allows hygromycin selection.

pNm2Hr carries a *mimp2* element into the first intron of the *niaD* gene and was constructed following the same steps as for the pNm1H18 construct (Dufresne et al. 2007). The *mimp2* copy corresponds to the reamplification of the *mimp2* element (AF076625) previously described (Hua-Van et al. 2000) using the HindImp primer (5′-GCCC TAAGCTTACAGTGGGGTGCAATAAGTTTG-3′). This primer anneals to the TIRs of *mimp2* and contains a *Hin*dIII site (underlined) at the 5′ end. PCR conditions were 1 min of denaturation at 95°C, followed by 30 cycles of 1 min 94°C, 1 min at 59°C, and 30 s at 72°C, then an elongation step of 10 min at 72°C. The PCR product was then digested with *Hin*dIII and inserted into the *Hin*dIII site of the first intron of *niaD* gene in plasmid pAN301 (Malardier et al. 1989), deleted of a dispensable *Nde*I fragment, resulting in the *niaD::mimp2* construct, also called pNm2Hr.

The artificial *mimp* element was generated using PCR in a three-step procedure. The first step used specific primers to amplify the desired genomic region, which will correspond to the central region of the artificial *mimp* element. The two others used chimeric primers, allowing the obtainment of a full-length artificial *mimp* with TIRs in two

successive PCR rounds. First, part of the first exon of the *F. oxysporum nia* gene, showing <50% identity to the orthologous sequence in *F. graminearum*, was amplified using primers niafox871+ (5′-ATACCCACAGCCTTCCT CCT-3′) and niafox1027– (5′-AGGACAGACTTTGGCG AG-3′) from genomic DNA of the FOM24 strain. PCR conditions were 5 min at 94°C, followed by 35 cycles of 1 min at 94°C, 1 min at 52°C, and 30 s at 72°C, and a final extension step of 10 min at 72°C. The eluted 157-bp PCR product was then used as template for amplification with the chimeric primers mimp_nia5′ (5′-AATAAGTTTGAAC GCC<u>ATACCCACAG</u>-3′) and mimp_nia3′ (5′-CAATAAG TTTGAATACC<u>AGGACAGACTTTG</u>-3′; the region complementary to the primary PCR product is underlined). PCR conditions were 5 min at 94°C, followed by 5 cycles of 1 min at 94°C, 1 min at 34°C, and 1 min at 72°C, then 30 cycles of 1 min at 94°C, 1 min at 62°C, and 1 min at 72°C, and a final extension step of 10 min at 72°C. The eluted PCR product was finally used as template in a final PCR with the HindImp primer (5′- GCCCT<u>AAGCTT</u>ACA GTGGGGTGCAATAAGTTTG-3′; *Hin*dIII restriction site underlined) under the following conditions: 5 min at 94°C, followed by 35 cycles of 1 min at 94°C, 1 min at 44°C, and 1 min at 72°C, and a final extension step of 10 min at 72°C. After all PCR steps, the eluted amplification product was cloned into the pGEM-T vector (Promega; Charbon-nières-les-Bains, France). After sequencing analysis of the whole product, the plasmid was digested with the *Hin*dIII restriction enzyme (see HindImp primer) and inserted into the *Hin*dIII site of the first intron of *niaD* gene in plasmid pAN301 as described above for the *niaD::mimp2*. The resulting construct was named pNmNia.

Transformation Experiments and Revertant Selection

Protoplast transformation was performed as previously described (Dufresne et al. 2007). Plugs of each cotrans-formant were picked on plates of nitrate minimal agar medium. Revertants were easily detected as patches of aerial mycelium with a wild-type phenotype on a background of sparse mycelium corresponding to a *niaD* mutant (see Fig. 4 in Dufresne et al. 2007).

DNA Preparation and Southern Blot Analysis

DNA extractions from *F. graminearum* strains were conducted as previously described (Dufresne et al. 2007). Ten micrograms of genomic DNA was digested with the appropriate restriction enzyme, separated electrophoretically on 0.7% agarose gels, and transferred on nylon membranes, using a vacuum blotter. DNA templates were

[32]P-labeled using the *redi*prime II kit (Amersham Biosciences). Hybridizations were conducted under standard conditions (Sambrook et al. 1989).

PCR and Primer Sequences

New *mimps* elements were amplified by PCR using the HindImp primer (see Plasmids and Contructs, under Materials and Methods section), under the same PCR conditions as described above, and genomic DNA of either the FOM24 or the FOL15 strain as template (50 ng per PCR reaction). Hybridization probes were obtained by PCR. The HindImp primer was used (PCR conditions: 1 min of denaturation at 95°C, followed by 30 cycles of 1 min at 94°C, 1 min at 59°C, and 30 s at 72°C, then an elongation step of 10 min at 72°C) to generate PCR products from different *mimp* elements. The 419-bp *niaD* probe was generated with primers niaDCG1 (5′-CACTA GTATGTGCAGGCAAC-3′) and niaDCG2 (5′-TTCAGCC ACTTGACACTG-3′), using the pAN301 plasmid as a template. PCR conditions were as follows: 2 min at 94°C, then 30 cycles of 30 s at 94°C, 30 s at 59°C, and 2 min at 72°C.

Excision events were controlled by PCR on 50 ng of genomic DNA of putative revertants and of the corresponding transformants, using primers niaD144 (5′-GT TCATGCCGTGGTCGCTGC-3′) and niaD754r (5′-AGT TGGGAATGTCCTCGTCG-3′) under the following conditions: 4 min at 94°C, then 30 cycles of 1 min at 94°C, 1 min at 59°C, and 2 min at 72°C. The sizes of the expected PCR products are 717 bp for a transformant and 485 bp for a revertant.

Amplification of Sequences Flanking *mimp* Elements

mimp2 flanking sequences were recovered using a modified TAIL-PCR approach as described for *mimp1* by Dufresne et al. (2007). The arbitrary degenerate (AD) primer AD2, 5′-AG(A/T)GNAG(A/T)ANCA(A/T)AGA-3′, and the specific primers, m2Tail1 (5′-GAATCCAGGCTGAAGTACC CG-3′) and m2Tail2 (5′-CCCGATTGGGGTATTGCTA TG-3′), were used with reduced-stringency and high-stringency annealing temperatures of 44°C and 63°C, respectively. To verify the duplication of a target site following transposition of *mimp*Nia, an inverse PCR strategy using the *Hae*III or *Xba*I restriction enzymes was carried out, using primers mniaDiv5 (5′-CTTTGCTGTTCCTGGAGGA G-3′) and mniaDiv3 (5′-TCTCGCCAAAGTCTGTCCT G-3′). PCR conditions were 5 min at 94°C, followed by 35 cycles of 1 min at 94°C, 1 min at 60°C, and 4 min at 72°C, and a final extension step of 10 min at 72°C.

Cloning of PCR Products and DNA Sequencing

PCR products were directly cloned into the pGEM-T vector (Promega) using 3 µl of either rough or purified PCR products, following the manufacturer's instructions. Sequencing of PCR products, either directly or cloned into the pGEM-T vector, was performed by Genome Express (Meylan, France) using an ABI Big Dye Terminator kit (Perkin Elmer) and the appropriate primer(s).

Computational Analysis

The design of optimal primers for PCR experiments was realized using the Primer3 program (http://primer3.sourceforge.net/). The quality of sequencing was visualized with the program Chromas Lite (http://www.technelysium.com.au/). The mfold algorithm (http://www.bioinfo.rpi.edu/applications/mfold/rna/form1.cgi) was used to visualize potential secondary structures formed by *mimp*-like elements as well as to determine their stability by calculating the ΔG_0 value. Blast analyses on the *F. oxysporum* and *F. graminearum* genomes were performed on the Fusarium Group web site, available at the Broad Institute (http://www.broad.mit.edu/annotation/genome/fusarium_group/MultiHome.html). For the determination of a potential consensus sequence of *mimp* insertions, 10 bp upstream and downstream of the target site was analyzed with the SeqLogo program (Schneider and Stephens 1990).

MITE Search by Complete Genome Screening

To perform an exhaustive MITE search, we used an ad hoc Perl script based on the following algorithm (available upon request). The nucleic acid sequence of each target TIR of a sequence length *l* were compared with the sequence of all sliding windows of the same length extracted from the *F. oxysporum* genome. A nucleotide polymorphism of 25%, slightly higher than the maximum value observed for TIRs examined manually (5 mismatches over 27 bp of TIRs), was tolerated. Once a candidate 5′-TIR was identified, a potential 3′-TIR was searched in a 500-bp range, in the range of maximum sizes usually reported for MITEs, with the same cutoff value of 75% identity. All MITE candidates were checked manually.

Phylogenetic Analysis

Multiple sequence alignments of the *mimp* nucleotidic sequences were performed using the MAFFT program using the default parameters (http://align.bmr.kyushu-u.ac.jp/mafft/online/server/). Alignments were then visualized using the sequence editor available in the MEGA4.0

package (Tamura et al. 2007). This package was also used to generate distance matrices and phylogenetic trees. The evolutionary history was inferred using the neighbor-joining method (Saitou and Nei 1987).

Results

Extracting *mimp*-Like Elements from the *F. oxysporum* Genome

In a previous work two different *mimp* elements had been identified by sequencing of genomic regions of the *F. oxysporum* FOM24 strain (*mimp1* and *mimp2* [Hua-Van et al. 2000]; accession numbers AF076624 and AF076625, respectively). These elements share the same structure: 27-bp *impalaE*-like TIRs, a central region with no coding capacity and exhibiting no homology with known sequences or between each other, and an overall size of ∼200–220 bp. To identify novel *mimp*-like elements, we conducted PCR experiments using a primer specific for part of the *impalaE* TIR sequence (HindImp; see Material and Methods section). After cloning of the rough PCR amplicon, 20 randomly chosen clones were analyzed by sequencing: 14 corresponded to *mimp1*-like elements, 3 to *mimp2*-like copies, and the 3 remaining sequences corresponded to two novel *mimp* elements called *mimp3* (two clones) and *mimp4* (one clone). *mimp3* exhibits *impalaE*-TIRs (Fig. 1) as *mimp1* and *mimp2* and is 216 bp long. The *mimp4* element, despite presenting a similar overall structure and size (220 bp), was shown, after BLASTN searches on the *F. oxysporum* genome sequence, to be characterized by the presence of *impalaF*-like TIRs (Fig. 1).

To determine the copy number of *mimp* elements in the genome of *F. oxysporum*, BLASTN searches were performed on the genome sequence recently available at the Broad Institute (http://www.broad.mit.edu/annotation/genome/fusarium_group/MultiHome.html) using the four *mimp* elements described above as templates. Following manual analysis of the BLASTN hits, 95 elements were identified. In the *F. oxysporum* genome, carrying several segmental duplications (L. J. Ma, Broad Institute; our laboratory, unpublished results), we removed redundant *mimp* copies. Among the 71 nonredundant elements, 58 could be assigned to one of the four known *mimp* subfamilies and 13 remained unclassified at this stage.
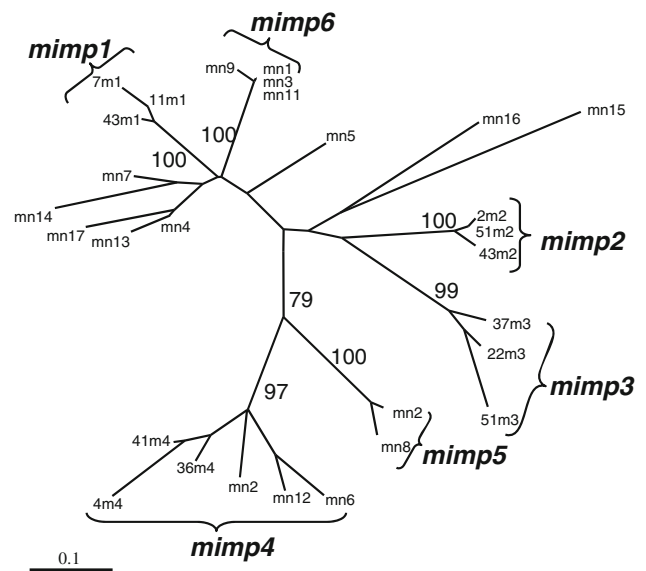
We wondered whether more divergent *mimp* elements could be missed by such a similarity-based search. We thus extended our analysis by developing a computer program based only on the search of similar TIR sequences (*impalaE*- or *impalaF*-TIRs) spaced by <500 bp (see Materials and Methods section). If other *mimp* subfamilies exist, this computer program should allow their detection without any

```
impE       5' CAGTGGGGTG CAATAAGTTTT GAATACA
impE       3' .......... .......... .......
mimp1ᵃ     5' .......A.. .......... ......C
mimp1ᵃ     3' .......A.. .......... ......C
mimp2      5' .......A.. .......... ...C..
mimp2      3' .......... .......... ...C..
mimp3      5' .....A.... .......... ...C..
mimp3      3' .......A.. ...G...... ....C..

impD       5' ........G. ...A....A. ....C..
impD       3' ........G. ...A....A. ....C..
mimp6      5' .......G. .......... A...G.C
mimp6      3' .......G. .......... G...C.C
mn16       5' .......G. .......... A...G.C
mn16       3' ....A...G. ...A...... A...C.C


impF       5' .......TC. ...A....A. TCGC.TCCAC
impF       3' .......T.. ...AT.C.A. TT-C..CCAC
mimp4ᵃ     5' .......A.. ...A....A. TCGC.GGTGT
mimp4ᵃ     3' .......A.. ...A....A. TCGG.GGTGT
mimp5      5' .......A.. .......A. TCGC.GGTGT
mimp5      3' .......A.. .......A. TCGC.TCCCA

mimp1ᵇ        .......... .......... ......C
mimp2ᵇ        .......... .......... ....C..
mimpNiaᵇ      .......... .......... ......C
```

Fig. 1 Comparison of TIR sequences of *mimp* elements with partial TIR sequences of *impala* elements belonging to subfamilies *E*, *D*, and *F*. The dots indicate identity to the reference sequence (*impE*, first 27 over 37 nt of the 5′ TIR). Differences are given by letters. The bar over the first sequence indicates nucleotides present in the HindImp primer used in PCR experiments (see Materials and Methods section). ᵃConsensus sequence determined from multiple sequence alignments of elements belonging to each subfamily. ᵇTIR sequences of the *mimp1*, *mimp2*, and *mimp*Nia elements used in cross-mobilization experiments. Due to their generation through PCR experiments using the same HindImp primer (see Materials and Methods section), these elements exhibit perfect TIRs whose sequences differ from the *impE* TIR one by a single nucleotide

Fig. 2 Optimal neighbor-joining tree obtained comparing a subset of sequences belonging to the four different known *mimp* subfamilies and the 17 additional sequences corresponding to novel *mimp* elements. Bootstrap values >60% supporting major clusters are shown. Distances are proportional to the evolutionary divergence expressed as substitutions per hundred sites. The optimal tree with the sum of branch lengths = 3.45663807 is shown. The evolutionary distances were computed using the maximum composite likelihood method (Tamura et al. 2004) and are given as the number of base substitutions per site (see scale). All positions containing gaps and missing data were eliminated from the dataset (complete deletion option). There were a total of 97 positions in the final dataset

a priori knowledge of the internal nucleotide sequence. We searched the complete *F. oxysporum* genome sequence and found eight additional *mimp* copies corresponding to four nonredundant sequences. Overall, 75 independent *mimp* copies were found in the whole *F. oxysporum* genome sequence, including 17 new *mimp* elements which could not be easily classified into any of the four known *mimp* subfamilies because they harbored completely different internal sequences.

To investigate further whether these new elements could define novel subfamilies, a subset of sequences including three full-length copies of each of the four *mimp1* to *mimp4* subfamilies and the 17 novel full-length *mimp* copies, called mn1 to mn17 (for *mimpnew*), was aligned using the MAFFT algorithm and the alignments used in phylogenetic analyses to obtain a neighbor-joining tree (Fig. 2). Six different monophyletic groups supported by high bootstrap values (>90%) were defined. These six distinct *mimp* subfamilies were called *mimp1* to *mimp6*. Apart from

isolated copies (mn5, mn15, and mn16; see Supplementary Table 1) corresponding to highly divergent sequences, a seventh group of sequences appeared on the phylogenetic tree (copies mn7, mn14, mn17, mn13, and mn4; see Supplementary Table 1). However, this group was not supported by >50% bootstrap values and was not considered significant. Considering the TIR sequences, three groups of *mimp* elements can be distinguished in the *F. oxysporum* genome. The first, comprised of the *mimp1*, *mimp2*, and *mimp3* subfamilies and most of the highly divergent *mimps* (*mn*), is characterized by the presence of *impalaE* TIRs. The second exhibits *impalaD* TIR sequences and comprises the *mimp6* subfamily as well as one divergent element, mn16. Finally, *mimp4* and *mimp5* subfamilies constitute a third group, characterized by *impalaF*-like TIRs.

Among the 75 identified *mimp* elements, we found both complete copies, referred to as full-length elements (Table 1), with TIRs and a target site duplication (TSD) sequence and truncated versions with only one discernible TIR. In all *mimp* subfamilies except *mimp5*, consisting of only two complete copies, full-length elements are largely predominant (Table 1). Only the 64 full-length copies were considered for further analysis.

Table 1 Sequence, size variability, and location relative to the closest predicted genes of the six *mimp* families

	Full-length	Truncated	Average nucleotide identity (%)	Location relative to closest predicted gene[a]			
				ORF	<500 bp	500–1000 bp	>1000 bp
mimp1	18	4	92.7%		39% (7)	28% (5)	33% (6)
mimp2	8	3	89.8%		25% (2)		75% (6)
mimp3	7	1	84.0%		28.5% (2)	28.5% (2)	43% (3)
mimp4	18	2	74.3%	5.5% (1)	5.5% (1)	28% (5)	61% (11)
mimp5	2	0	92.1%				100% (2)
mimp6	4	1	97.9%			50% (2)	50% (2)
Other *mimps*	7	0	n.d.			71.4% (5)	28.6% (2)
Total	64	11	n.d.	1.6% (1)	18.7% (12)	29.7% (19)	50% (32)

[a] To determine the distance of *mimp* reinsertion sites to genes, the annotated version of the *F. oxysporum* genome sequence was used; it is available at the Broad Institute web site (http://www.broad.mit.edu/annotation/genome/fusarium_group/MultiHome.html)

Nucleotide polymorphism was examined and showed that all *mimp* subfamilies are characterized by a high level of nucleotide identity (92–98%), even if the *mimp4* subfamily exhibits a higher level of sequence variation (25%). Another striking characteristic of *mimp* elements is their remarkable size homogeneity (between 204 and 226 bp). Apart from *mimp* elements, our computer-based search identified two already known deleted versions of *impalaD* (367 and 471 bp, respectively [Hua-Van et al. 2001a; unpublished results]).

Mobilization of a Native and a De Novo Created mimps by the *impalaE* Transposase

We have previously demonstrated that the native *mimp1* element could be mobilized by the *impalaE* transposase (Dufresne et al. 2007). Since sequence similarity between *mimp1* and *impalaE* is restricted to the TIRs, mobilization of other elements sharing similar TIRs would be expected. However, cross-mobilization is not fully predictable since we do not know the role of sequences in the central region. To determine if similarity in the TIRs is the only requirement or if the central region contributes to the transposition process, we evaluated the cross-mobilization by the *impalaE* transposase of both a *mimp2* element and a de novo created *mimp*, *mimp*Nia, according to the same procedure as the one already developed for *mimp1*, in the heterologous *F. graminearum* genetic background (Dufresne et al. 2007).

Five cotransformants, carrying both the *mimp2* element inserted into the *niaD* gene and the construct allowing expression of the source of *impala* transposase, were obtained and replicated each on three minimal medium plates (see Materials and Methods section) to test for *mimp2* excision. Based on the phenotypic assay, colonies which grew aerial were considered as revertants resulting from excision of *mimp2*. All five cotransformants gave a high rate of excision (20 to >100 revertants per plate; Table 2). A set of 12 potential revertants was analyzed by Southern blot to confirm *mimp2* excision and estimate reinsertion rates. The results indicated that all revertants correspond to an excision event (Fig. 3a, top). Sequencing of the empty sites revealed, in all cases, a footprint of five additional nucleotides, two corresponding to the duplication of the TA target site and three to one of the ends of the element, as already observed for *impala* (Hua-Van et al. 2001b) and *mimp1* (Dufresne et al. 2007) (data not shown). Using the *mimp2* element as a probe (Fig. 3a, bottom, and Table 2), reinsertion was observed in 50% (6/12) of the strains analyzed, a frequency which appears to be lower than that observed for *mimp1* in the same genetic background (95% [Dufresne et al. 2007]).

Table 2 Sizes, predicted ΔG_0 values, and transposition efficiencies of native *mimp1* and *mimp2* and the artificial *mimp*Nia element

mimp element	Size (bp)	ΔG_0 with TIRs (kcal/mol)	Excision[a]	Reinsertion
mimp1	224	−80.50	20–100	95% (23/24)[b]
Mimp2	213	−87.69	20–100	50% (6/12)[c]
mimpNia	211	−59.07	1–2	27% (3/11)[c]

[a] Number of Nia[+] colonies detected per minimal medium agar plate (see Materials and Methods section)

[b] Determined by PCR using *mimp1*-specific primers (Dufresne et al. 2007)

[c] Determined by Southern blot analysis using a *mimp2*- or *mimp*Nia-specific probe, respectively

To further test the impact of *mimps* central region, we constructed an artificial *mimp* element in vitro, exhibiting the following structure: typical 27-bp *impalaE*-like TIRs and a central region, giving an overall size of 211 bp. We selected a region in the first exon of the *F. oxysporum nia* gene showing low homology with the *F. graminearum* genome. The corresponding *mimp* element was called *mimp*Nia. The size and ΔG_0 value for the *mimp*Nia element compared with those of *mimp1* and *mimp2*, with and without TIRs, are presented in Table 2. This element was then introduced into the first intron of the *A. nidulans niaD* gene leading to plasmid construct pNmNia (see Materials and Methods section). Among eight cotransformants carrying the pNmNia construct, two (N4 and N5) gave rise to only a few Nia$^+$ colonies (one or two per plate; Table 2) within a 4- to 6-week incubation time. To evaluate the behavior of the artificial *mimp*, Southern blot experiments were conducted. A set of 11 revertants, resulting from the excision of *mimp*Nia, was analyzed. Hybridizing bands observed using the *niaD* probe (Fig. 3b; top) showed that they all correspond to excision events. Sequencing of the corresponding empty sites showed that eight of them exhibited typical excision footprints as already found for native *mimp1* and *mimp2* elements (Fig. 4). In the three remaining cases, more or less extended deletions were observed (Fig. 4). These modifications (typical excision footprints or deletions) do not alter splicing of the *niaD* intron, explaining why a wild-type nitrate-reductase activity was restored in these strains. Concerning the fate of the excised copy, the use of the *mimp*Nia element as a probe showed reinsertion in at least three cases (lanes 2, 3, and 11 in Fig. 3b, bottom, and Table 2).

Altogether, these results demonstrate that *mimp2* and also the in vitro created *mimp*Nia element can be transactivated by the *impalaE* transposase and transpose through a canonical "cut-and-paste" mechanism. However, looking in more detail at the different steps in the transposition process, some differences are observed. The *mimp2* element differs from *mimp1* only by a less frequent reinsertion of the excised copy (Table 2). In contrast, the overall transposition efficiency of the *mimp*Nia element is highly reduced: excision events are rare and <30% of the excised copies reinsert in the genome (Table 2). These results suggest that if TIR sequences are the minimal requirement for mobilization by the *impalaE* transposase through a cut-and-paste mechanism, additional parameters are likely required for efficient transposition.

Genomic Organization and Insertion Sites of *mimp* Elements

Looking at the distribution of *mimp* elements on the 15 *F. oxysporum* chromosomes, a strong bias was revealed
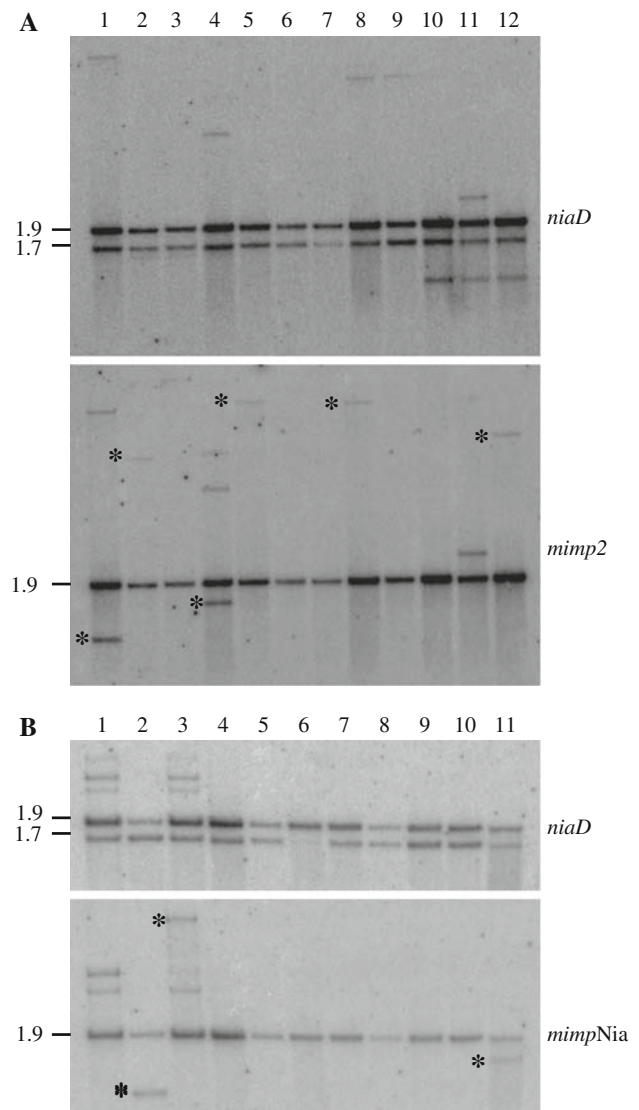
Fig. 3 Southern blot analysis of a set of potential *mimp2* revertants **a** and *mimp*Nia revertants **b** in the *F. graminearum* Fg820 genetic background. Genomic DNA was digested with *Xba*I and the membrane was successively hybridized with an *niaD* probe (*top*) and a *mimp2* or *mimp*Nia probe (*bottom*). The stars in the bottom panel indicate the reinsertion of excised copies. The presence of a 1.7-kb hybridization band using the *niaD* probe indicates an excision event. Using the same probe, the detection of a 1.9-kb hybridization band, and, in some cases, additional hybridization bands, further indicates that the original cotransformants carry more than one copy of the *niaD::mimp* construct

(Fig. 5a), with seven chromosomes containing no *mimp* element and one, chromosome 14, carrying nearly 50% of the copies (48/103; Fig. 5a). This biased distribution is not due to one specific *mimp* subfamily but is rather a tendency for all *mimp* elements (data not shown). No strict correlation between the distribution of *mimp* and that of *impala* elements could be established (Fig. 5a) since chromosomes were found carrying *mimps* and no *impala* (chromosome

```
n=7 CGAAAAGCTTACag............................TAAGCTTACAG
n=3 CGAAAAGCTTA............................ctgTAAGCTTACAG
n=2 CGAAAAGCTTA............................        CAG
n=1 CGAAAAGCTTAcagtggggtgcaataagtttga.....actgTAAGCTTACAG
```

Fig. 4 Structure of *mimp*Nia excision sites in *F. graminearum* revertants. The TA dinucleotide target site is indicated in boldface. Nucleotide insertions or deletions relative to the *niaD* sequence without the *mimp*Nia element are framed. n: number of revertants exhibiting the indicated nucleotide sequence
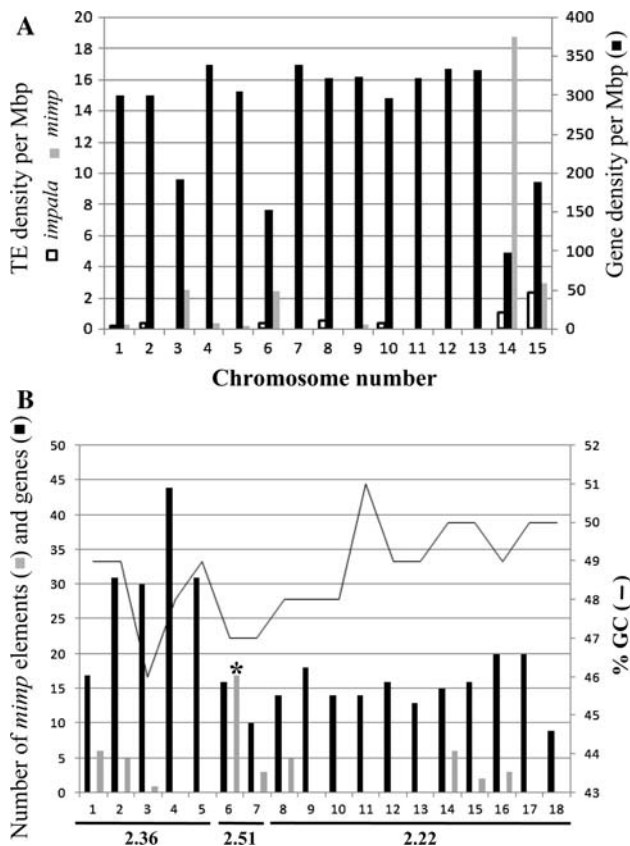
Fig. 5 a Relative densities of the annotated *impala* and *mimp* elements and of genes on the 15 chromosomes of *Fusarium oxysporum*. **b** Detailed analysis of the distribution of genes and *mimp* elements and of the GC content on chromosome 14. Numbers 1 to 18 correspond to 100-kbp intervals, with the exception of intervals 5 (superconting 2.36, positions 400,001–480,600), 7 (supercontig 2.51, positions 100,001–133,248), and 18 (supercontig 2.22, positions 1,000,001–1,030,612). The asterisk indicates the interval in which a concentration of *mimp* elements was observed (17 copies over 48 annotated on this chromosome)

3), and vice versa (chromosomes 2 and 8). However, a higher density of both elements was noticed on chromosome 14 (Fig. 5a). To explain this bias, we examined the gene content of the 15 chromosomes. As shown in Fig. 5a, four chromosomes are characterized by a relative paucity of genes. Among them, chromosome 14 is the only one exhibiting such a high concentration of *mimp* elements. Looking in more detail at the location of *mimp* elements on

chromosome 14, we noticed that insertion sites are not random. Half of the copies (22/48) cluster together, spaced by 40 bp to 22 kbp, most of them being located in a 100-kbp interval on supercontig 2.51 (Fig. 5b). No relationship with either gene density or TA content could be established to explain the concentration of *mimp* elements on this interval (Fig. 5b). One *mimp4* element was found inserted within a *mimp3* copy.

To analyze *mimp2* insertional preference in the *F. graminearum* genome, we performed a systematic recovery of flanking sequences using tail PCR. After sequencing, BLASTN searches on the *F. graminearum* genome sequence were used to locate 42 independant reinsertion sites, according to the third release of the assembled and annotated genome, available in the *Fusarium* Group database at the Broad Institute (http://www.broad.mit.edu/annotation/genome/fusarium_group/MultiHome.html). Most insertions were unique (34/42), however, four were hit twice. In contrast to the observations for native *mimps* in the *F. oxysporum* genome, the 38 independent *mimp2* reinsertion sites seem to occur rather randomly over the four *F. graminearum* chromosomes, even though a slight bias is revealed on chromosomes 2 and 4, with fewer insertions observed than expected on chromosome 2 and more on chromosome 4 (Table 3).

The analysis of 60 nt around the insertion site of both the 64 independent full-length *mimp* elements in *F. oxysporum* and the 38 independent *mimp2* reinsertion sites in *F. graminearum* revealed that, in addition to the TA dinucleotide target site, no consensus sequence could be found at *mimps* insertion sites. However, *mimp* elements tend to target genomic regions enriched in A/T nucleotides. For native *mimps*, the AT content of insertion sites varies from 56.3% (*mimp1* subfamily) to 65.5% (*mimp5* subfamily), whereas the average value for the *F. oxysporum* genome is 51.6%, reaching 54.6% in noncoding regions (http://www.broad.mit.edu/annotation/genome/fusarium_group/MultiHome.html). Similar results were found when analyzing *mimp2* reinsertion sites in the *F. graminearum* genome (data not shown).

Table 3 Observed and expected numbers of *mimp2* insertions on the four *F. graminearum* chromosomes: calculations were made assuming that all TA dinucleotides are equally accessible

	Chromosome				Total
	1	2	3	4	
TA targets	543,481	431,023	360,659	372,165	1,707,328
Insertions Observed	17[a]	4[a]	8	13[a]	42
Expected	13	11	9	9	42

[a] Chi-square test, $p \leq 0.05$

To determine whether the targeting of AT-rich regions correlates with a preferential location in noncoding regions, we analyzed the regions flanking the 64 full-length *mimp* elements and calculated the distance toward the closest predicted gene in the *F. oxysporum* genome. One and six-tenths percent of the copies lie within a predicted gene (one element in an intronic region), 18.7% lie <500 bp from an ORF, and 29.7% lie >500 and <1000 bp from an ORF (Table 1), while the average intergenic distance in the *F. oxysporum* genome is 1974 bp. The location of *mimp* endogenous elements varies from one subfamily to another. For example, whereas *mimp4* elements are located predominantly far from genes (only 11% at <500 bp from an ORF; see Table 1), *mimp1* elements are closer to genes (nearly 40% at <500 bp from an ORF; see Table 1). A similar analysis of *mimp2* reinsertion sites in the cross-mobilization assay showed that more than 45% (18/38) were found to be within (3/38) or in the close vicinity of (<500 bp upstream or downstream [15/38]) predicted genes (Table 4), with a preference for 5′-regions (11 vs. 4 insertions in the 5′- and 3′-regions, respectively). These results are very similar to those observed for *mimp1* in the same genetic background (Dufresne et al. 2007; unpublished results).

Discussion

In this study we took advantage of the recent availability of the *F. oxysporum* genome sequence to perform a genome-wide analysis of the *mimp* elements, a family of MITEs for which a few members had previously been identified in this fungal species (Hua-Van et al. 2000). Two approaches were developed. The first consisted in using sequences of two known *mimp* elements, *mimp1* and *mimp2* (Hua-Van et al. 2000), and of two novel *mimp3* and *mimp4* elements identified by a PCR approach (this study) as queries in standard BLASTN searches (Altschul et al. 1997). This analysis allowed the identification of both full-length and truncated copies. However, divergent *mimp* elements could have been missed in such a similarity-based search. We thus extended our analysis by developing a computer program based only on the presence of similar TIR sequences (75% nucleotide identity) spaced by <500 bp, to extract all *mimp* elements in the genome of *F. oxysporum*. Similar strategies have been conducted in other eukaryote genomes such as *Arabidopsis thaliana* to analyze the *Emigrant* family (Santiago et al. 2002) and *Anopheles gambiae* (Tu 2001).

Table 4 *mimp2* reinsertion sites located <500 bp from a *F. graminearum* predicted gene

Revertant	*F. graminearum* supercontig DNA giving BLASTN hit[a]	Closest predicted ORF	Distance to *mimp2* (bp)
1.2	7 (104,703)	FGSG_09890	282 (5′)
1.4	6 (1,648,029)	FGSG_09460	88 (3′)
1.21	8 (832,103)	FGSG_10945	123 (5′)
1.24	1 (5,126,928)	FGSG_01565	34 (3′)
2.1	8 (1,436,055)	FGSG_13922	121 (5′)
2.4–3.14	8 (478,806)	FGSG_11066	ORF
2.15	3 (1,268,782)	FGSG_05136	8 (5′)
3.10	1 (904,282)	FGSG_00299	456 (5′)
3.12	10 (159,677)	FGSG_11569	12 (3′)
3.17–4.7	1 (6,755,548)	FGSG_02064	378 (5′)
4.2	2 (5,196,680)	FGSG_02854	ORF
4.5	4 (2,099,966)	FGSG_07039	342 (5′)
4.9	1 (6,578,218)	FGSG_12054	420 (5′)
4.10	4 (2,857,291)	FGSG_13104	479 (3′)
4.11	6 (2,534,854)	FGSG_09727	ORF
4.12–4.22	1 (1,317,558)	FGSG_00421	264 (5′)
5.2	3 (4,202,475)	FGSG_06068	328 (5′)
5.14	1 (4,102,270)	FGSG_11917	437 (5′)

Note: The BlastN algorithm (Altschul et al. 1997) was used to search for significant matches in the *Fusarium graminearum* genome database at the Broad Institute (http://www.broad.mit.edu/annotation/genome/fusarium_group/MultiHome.html)

[a] Supercontig DNA from the *F. graminearum* genome sequence giving a hit with *mimp2* flanking sequences. The location of the *mimp2* insertion in each contig DNA is indicated in parentheses. To determine the distance of *mimp2* reinsertion sites to genes, the annotated version of the *F. graminearum* genome sequence, available at the Broad Institute (see the Internet address above), was used. Column 3 indicates the closest predicted gene to the *mimp2* insertion site. The relative *mimp2* location is then indicated as follows: 5′, 3′, and ORF indicate positions (nt) within the 5′ region, 3′ region, or coding sequence of the gene, respectively

Overall, our analysis identified 103 *mimp* copies. This number could appear to be unusually low in comparison with most MITE families in plant and animal species. However, considering the size of the *F. oxysporum* genome (60 Mb), it is in the same range as that observed for the *Emigrant* family of MITEs in *Arabidopsis* (Santiago et al. 2002). Forty-three *mimp* elements were found in two to five identical copies, being part of larger redundant genomic regions. A phylogenetic analysis conducted on a subset of *mimp* copies showed that *mimp* elements belong to at least six different subfamilies, called *mimp1* to *mimp6*. Eight *mimp* copies are too divergent to be included in any of the six defined subfamilies. Nevertheless, *mimp* full-length elements share common characteristics: *impala*-like TIRs, which may, depending on the subfamily, be more similar to *impalaE* (*mimp1, mimp2, mimp3*), *impalaD* (*mimp6*), or *impalaF* (*mimp4, mimp5*) TIR sequences, and a very homogeneous size, ranging between 204 and 226 bp. *Tourist* and *Stowaway*, two large plant MITE families, also exhibited this remarkable length homogeneity (Bureau and Wessler 1992, 1994a). Since then, size homogeneity has been found to be one of the characteristics of MITEs that distinguish them from other nonautonomous elements (Wessler et al. 1995). *mimp* subfamilies exhibit different degrees of variability. Whereas *mimp1* and *mimp6* are very homogeneous (93% and 98% nucleotide identity, respectively), elements belonging to the *mimp4* subfamily are more divergent from one another (74% nucleotide identity). This suggests that different amplification bursts, each starting from a distinct *mimp* element and occurring at different times, gave rise to these subfamilies. The absence of any active copy of *impala*, the *mimp* autonomous partner (Dufresne et al. 2007; this work), in this genome prevents further amplification of *mimps* at this stage (M. Dufresne and M. J. Daboussi, unpublished results). However, different situations might be encountered in other *F. oxysporum* strains in which potentially active members of the *impala* family are still present (Hua-Van et al. 2001a).

A strong bias of distribution of endogenous *mimp* elements was revealed, whatever *mimp* subfamily, when looking at their insertion sites along the 15 *F. oxysporum* chromosomes. Seven chromosomes do not contain any *mimp* element, whereas chromosome 14 carries 46.6% of the 103 identified *mimp* copies. The density of *mimp* elements on chromosome 14 is two to seven times higher than that observed for TEs belonging to other superfamilies (L. J. Ma, Broad Institute; our laboratory, unpublished results). Detailed analysis of the distribution on this chromosome revealed that *mimp* elements tend to group together, as nearly half of the copies are found adjacent, as close as 40 bp. Only a single case of a *mimp* insertion into another *mimp* was observed, a situation different from that reported for *Tourist* MITEs (Jiang and Wessler 2001). The

enrichment in *mimps* on this chromosome, contrary to the observations on other chromosomes such as chromosomes 3 and 6, is not due to the occurrence of segmental duplications. TEs have been reported to accumulate in some genomic regions, such as heterochromatin. However, the concentration of nearly half of *mimp* copies in such a small region of the genome is outstanding. The only element for which such a peculiar distribution was observed is the *Bari1* transposon of *Drosophila*. This element is present in *D. melanogaster* both as single-copy elements scattered in the euchromatin and as a discrete cluster in the heterochromatin (Marsano et al. 2003). The similar distribution of *mimp* and *Bari1* elements could suggest that the *F. oxysporum* genomic region in which *mimp* elements are found concentrated may be in the process of heterochromatinization. Alternatively, this distribution may result from local hopping of *mimps* elements, a phenomenon already described for other transposons such as the *P*, *Ac*, and *Sleeping Beauty* elements (Mátés et al. 2007). However, such a behavior has never been reported for the master element *impala* in *F. oxysporum*, in which reinsertion has been shown to occur randomly (Migheli et al. 2000). Moreover, the *mimp1* and *mimp2* elements do not exhibit such an insertion bias in the heterologous species *F. graminearum* (Dufresne et al. 2007; this work).

Plant MITE families have often been found associated with genes (Bureau and Wessler 1992, 1994a, b; Bureau et al. 1996; Yang et al. 2001; Han and Korban 2007). The distribution of *mimp* elements belonging to the six different subfamilies with respect to predicted genes was examined. On average, *mimp* elements were found far from genes, with more than 75% of the insertions located >500 bp from the closest ORF (see Table 1). However, this insertional preference was far less pronounced for the *mimp1* subfamily, in which nearly 40% of the insertions were found <500 bp from a predicted ORF. A general tendency could be that *mimp* elements close to genes have been eliminated during evolution. This phenomenon is expected to be less apparent for more recent elements, such as those belonging to the very homogeneous *mimp1* subfamily. Our results are in contrast with the analysis conducted on the *Emigrant* family of MITEs in *Arabidopsis*, in which copies close to genes were shown to have been maintained during evolution (Santiago et al. 2002).

In analysis of the location of newly mobilized *mimp2* elements toward predicted genes in *F. graminearum*, we obtained a rather different picture. Nearly half of the insertions were found <500 bp from a predicted ORF. This result may reflect the propensity of *mimp2* to target genic regions and thus favor the hypothesis that *mimp* elements, including endogenous *mimp2* elements, close to genes have been negatively selected during the evolution of the genome of the *F. oxysporum* sequenced strain. Alternatively, the

observed discrepancy between insertional preference of endogenous *mimp2* elements in *F. oxysporum* and newly transposed *mimp2* copies in *F. graminearum* could be due to structural differences between the two genomes. The genome of *F. graminearum* is characterized by a high gene density and a remarkable paucity in repeated sequences (Cuomo et al. 2007). In contrast, *F. oxysporum* genome exhibits a high expansion of repeated sequences together with the occurrence of several large segmental duplications.

In a previous study, we demonstrated that *mimp1* could be mobilized through the action of the transposase of *impalaE*, a *Tc1*-like autonomous element (Dufresne et al. 2007). Genome-wide analysis of the *mimp* elements in *F. oxysporum* showed that a number of them have TIRs similar to those of the autonomous *impalaE* element. To further evaluate the potential of *impalaE* to mobilize *mimp* elements as well as to evaluate the impact of sequences of the central region of *mimp* elements, we used a second native *mimp* element, *mimp2*, and an in vitro created *mimp* element, *mimp*Nia, both carrying *impalaE*-like TIR sequences, in transactivation experiments. We demontrated that *mimp2* and *mimp*Nia are mobilized by the *impalaE* transposase, and transpose through a "cut-and-paste" mechanism, providing evidence that *impalaE* is the autonomous partner of different *mimp* subfamilies.

However, transposition efficiencies appear to be lower than that observed for the native *mimp1* element, in particular, for the *mimp*Nia element, for which a drastic reduction in both excision and reinsertion was observed. The TIR sequences of the three *mimp* elements tested so far in our transposition assay differ by only a single nucleotide from *impE* TIR sequences, and the *mimp1* and *mimp*Nia elements exhibit identical TIRs. Therefore, even if TIR sequences appear to be the main requirement for *mimp* mobilization, these results suggest that the internal sequence might influence transposition efficiency. Results of binding experiments between the *Lemi1* transposase and *Emigrant* MITEs showed that subterminal repeated motifs are important for transposase interaction and, possibly, for mobilization of these elements (Loot et al. 2006). No such sequence feature was found in *mimp1* and *mimp2*, the two native *mimp* elements for which mobilization has been demonstrated. Another parameter that could explain the difference in transposition efficiency is the lower potential of the element we created to form a stable secondary structure. However, this does not stand for *mimp2*, which exhibits as *mimp1* a strong potential to form a stable secondary structure. Deciphering which parameters are crucial for efficient transposition will be investigated further. One way would be to construct *mimp* elements corresponding either to chimera or to mutated versions of native *mimp* elements and to compare their transposition efficiency. However, to ensure a proper quantitative comparison, this will require assignment of the different constructs to the same genomic locus to avoid some of the variations observed being due to the effect of donor loci.

The relationships between *mimp* elements and *impala* autonomous members will also be analyzed further. Our exhaustive analysis of *mimp* elements in *F. oxysporum* has shown that three groups of *mimps* are found carrying TIRs resembling those of *impalaE*, *impalaD*, or *impalaF*, respectively. The potential of autonomous elements other than *impalaE* to mobilize different *mimps* will be tested. Previous studies have shown that *impalaD*, the only other available autonomous copy of *impala*, can cross-mobilize defective *impalaE* elements (Hua-Van et al. 2001b). A similar result is expected for *mimp* elements exhibiting TIRs similar to *impalaE*. Testing whether cross-mobilization of *mimps* carrying more divergent *impalaF* TIRs can occur will be of particular interest.

References

Altschul SF, Madden TL, Schäffer AA, Zhang J, Zhang Z, Miller W, Lipman DJ (1997) Gapped BLAST and PSI-BLAST: a new generation of protein database search programs. Nucleic Acids Res 25:3389–3402

Bai G, Shaner G (1996) Variation in *Fusarium graminearum* and cultivar resistance to wheat scab. Plant Dis 80:975–979

Bureau TE, Wessler SR (1992) *Tourist*: a large family of small inverted repeat elements frequently associated with maize genes. Plant Cell 4:1283–1294

Bureau TE, Wessler SR (1994a) Mobile inverted-repeat elements of the *Tourist* family are associated with the genes of many cereal grasses. Proc Natl Acad Sci USA 91:1411–1415

Bureau TE, Wessler SR (1994b) *Stowaway*: a new family of inverted repeat elements associated with the genes of both monocotyledonous and dicotyledonous plants. Plant Cell 6:907–916

Bureau TE, Ronald PC, Wessler SR (1996) A computer-based systematic survey reveals the predominance of small inverted-repeat elements in wild-type rice genes. Proc Natl Acad Sci USA 93:8524–8529

Carroll AMC, Sweigard JA, Valent B (1994) Improved vectors for selecting resistance to hygromycin. Fungal Genet Newslett 41:22

Cuomo CA, Güldener U, Xu JR, Trail F, Turgeon GB, Di Pietro A, Walton JD et al (2007) The *Fusarium graminearum* genome reveals a link between localized polymorphism and pathogen specialization. Science 317:1400–1402

Daboussi MJ, Capy P (2003) Transposable elements in filamentous fungi. Annu Rev Microbiol 57:275–299

Dufresne M, Hua-Van A, Abd el Wahab H, Ben M'Barek S, Vasnier C, Teysset L, Kema GHJ, Daboussi MJ (2007) Transposition of a fungal miniature inverted-repeat transposable element through the action of a *Tc1*-like transposase. Genetics 175:441–452

Feschotte C, Mouches C (2000) Evidence that a family of miniature inverted-repeat transposable elements (MITEs) from the *Arabidopsis thaliana* genome has arisen from a *pogo*-like DNA transposon. Mol Biol Evol 17:730–737

Feschotte C, Zhang X, Wessler SR (2002) Miniature inverted-repeat transposable elements in their relationship to established DNA transposons. In: Craig NL, Craigie R, Gellert M, Lambowitz AM (eds) Mobile DNA II. American Society of Microbiology, Washington, DC, pp 1147–1158

Feschotte C, Swamy L, Wessler SR (2003) Genome-wide analysis of *mariner*-like transposable elements in rice reveals complex relationships with *Stowaway* miniature inverted repeat transposable elements (MITEs). Genetics 163:747–758

Feschotte C, Osterlund MT, Peeler R, Wessler SR (2005) DNA-binding specificity of rice mariner-like transposases and interactions with *Stowaway* MITES. Nucleic Acids Res 33:2153–2165

Han Y, Korban SS (2007) *Spring*: an novel family of miniature inverted-repeat transposable elements is associated with genes in apple. Genomics 90:195–200

Hua-Van A, Héricourt F, Capy P, Daboussi MJ, Langin T (1998) Three highly divergent subfamilies of the *impala* transposable element coexist in the genome of the fungus *Fusarium oxysporum*. Mol Gen Genet 259:354–362

Hua-Van A, Davière JM, Langin T, Daboussi MJ (2000) Genome organiziation in *Fusarium oxysporum*: clusters of class II transposons. Curr Genet 37:339–347

Hua-Van A, Langin T, Daboussi MJ (2001a) Evolutionary history of the *impala* transposon in *Fusarium oxysporum*. Mol Biol Evol 18:1959–1969

Hua-Van A, Pamphile JA, Langin T, Daboussi MJ (2001b) Transposition of autonomous and engineered *impala* transposons in *Fusarium oxysporum* and a related species. Mol Gen Genet 264:724–731

Jiang N, Wessler SR (2001) Insertion preference of maize and rice miniature inverted repeat transposable elements as revealed by the analysis of nested elements. Plant Cell 13:2553–2564

Jiang N, Bao Z, Zhang X, Hirochika H, Eddy SR, McCouch SR, Wessler SR (2003) An active DNA transposon family in rice. Nature 421:163–167

Kikuchi K, Terauchi K, Wada M, Hirano HY (2003) The plant MITE *mPing* is mobilized in anther culture. Nature 421:167–170

Loot C, Santiago N, Sanz A, Casacuberta JM (2006) The proteins encoded by the pogo like Lemi1 element bind the TIRs and subterminal repeated motifs of the *Arabidopsis Emigrant* MITE: consequences for the transposition mechnism of MITEs. Nucleic Acids Res 34:5238–5246

Macas J, Koblizkova A, Neumann P (2005) Characterization of *Stowaway* MITEs in pea (*Pisum sativum* L.) and identification of their potential master elements. Genome 48:831–839

Malardier L, Daboussi MJ, Julien J, Roussel F, Scazzocchio C et al (1989) Cloning of the nitrate reductase gene (*niaD*) of *Aspergillus nidulans* and its use for transformation of *Fusarium oxysporum*. Gene 78:147–156

Marsano RM, Milano R, Minervini C, Moschetti R, Caggese C, Barsanti P, Caizzi R (2003) Organization and possible origin of the *Bari-1* cluster in the heterochromatic h39 region of *Drosophila melanogaster*. Genetica 117:281–289

Mátés L, Izsvak Z, Ivics Z (2007) Technology transfer from worms and flies to vertebrates:transposition-based genome manipulations and their future perspectives. Genome Biol 8(Suppl I):S11–S119

Migheli Q, Steinberg C, Davière JM et al (2000) Recovery of mutants impaired in pathogenicity after transposition of *Impala* in *Fusarium oxysporum* f. sp. *melonis*. Phytopathology 90:1279–1284

Quesneville H, Nouaud D, Axolabéhère D (2006) *P* elements and MITE relatives in the whole genome sequence of *Anopheles gambiae*. BMC Genom 7:214–227

Ramussen JP, Taylor AH, Ma LJ, Purcell S, Kempken F, Catcheside DE (2004) *Guest*, a *transposable* element belonging to the *Tc1/mariner* superfamily is an ancient invader of *Neurospora* genomes. Fungal Genet Biol 41:52–61

Saito M, Yonemaru J, Ishikawa G, Nakamura T (2005) A candidate autonomous version of the wheat MITE *Hikkoshi* is present in the rice genome. Mol Genet Genom 273:404–414

Saitou N, Nei M (1987) The neighbor-joining method: a new method for reconstructing phylogenetic trees. Mol Biol Evol 4:406–425

Sambrook J, Fritsch EF, Maniatis T (1989) Molecular cloning: a laboratory manual. Cold Spring Harbor Laboratory, Cold Spring Harbor, NY

Santiago N, Herraiz C, Goni JR, Messeguer X, Casacuberta JM (2002) Genome-wide analysis of the *Emigrant* family of MITEs of *Arabidopsis thaliana*. Mol Biol Evol 19:2285–2293

Schneider TD, Stephens RM (1990) Sequence logos: a new way to display consensus sequences. Nucleic Acids Res 18:6097–6100

Tamura K, Nei M, Kumar S (2004) Prospects for inferring very large phylogenies by using the neighbor-joining method. Proc Natl Acad Sci USA 101:11030–11035

Tamura K, Dudley J, Nei M, Kumar S (2007) MEGA4: Molecular Evolutionary Genetics Analysis (MEGA) software, version 40. Mol Biol Evol 24:1596–1599

Tu Z (2001) Eight novel families of miniature inverted repeat transposable elements in the African malaria mosquito, *Anopheles gambiae*. Mol Biol Evol 98:1699–1704

Wessler SR, Bureau TE, White SE (1995) LTR-retrotransposons and MITEs: important players in the evolution of plant genomes. Curr Opin Genet Dev 5:814–821

Yang G, Dong J, Chandrasekharan MB, Hall TC (2001) *Kiddo*, a new transposable element family closely associated with rice genes. Mol Genet Genom 266:417–424

Yang G, Zhang F, Hancock CN, Wessler SR (2007) Transposition of the rice miniature inverted repeat transposable element *mPing* in *Arabidopsis thaliana*. Proc Natl Acad Sci USA 104:10962–10967